2-6-2012

Highly Piezoelectric Biocompatible and Soft Composite Fibers

J. Morvan
Kent State University - Kent Campus

E. Buyuktanir
Kent State University - Kent Campus

John L. West
Kent State University - Kent Campus

Antal Jakli
Kent State University - Kent Campus, ajakli@kent.edu

Highly piezoelectric biocompatible and soft composite fibers

J. Morvan,[1] E. Buyuktanir,[2,3] J. L. West,[2,4] and A. Jákli[1,2,a)]
[1]*Chemical Physics Interdisciplinary Program, Kent State University, Kent, Ohio 44242, USA*
[2]*Liquid Crystal Institute, Kent State University, Kent, Ohio 44242, USA*
[3]*Department of Chemistry, Stark State College, North Canton, Ohio 44720, USA*
[4]*Department of Chemistry, Kent State University, Kent, Ohio 44242, USA*

(Received 28 September 2011; accepted 15 January 2012; published online 8 February 2012)

We report the fabrication of highly piezoelectric biocompatible soft fibers containing barium titanate ferroelectric ceramic particles dispersed in electrospun poly lactic acid (PLA). These fibers form mats that have two orders of magnitude larger piezoelectric constant per weight than single crystal barium titanate films. We propose that the observed apparent piezoelectricity results from the electrospinning induced polar alignment of the ferroelectric particles that pole the fibers similar to ferroelectret polymer foams that are poled by corona discharge. Due to the biocompatibility of PLA that encases the ferroelectric particles, these mats can be used in biological applications such as bio-sensors, artificial muscles, and energy harvesting devices. © *2012 American Institute of Physics*. [doi:10.1063/1.3683482]

Piezoelectricity (a linear coupling between electric and mechanical signals) was discovered in non centro-symmetric crystals by the Curie brothers in 1880.[1] Since then piezoelectricity has been observed in ceramics,[2] certain synthetic[3] and biological polymers,[4,5] and ferroelectric liquid crystals.[6,7] Today piezoelectric materials are used in ultrasonic and hydroacoustic devices,[8] for frequency standards,[9] and in electromechanical actuators and sensors.[10] Recently certain cellular polymers internally charged by corona discharge (ferroelectrets) have been found to behave like soft sensitive piezoelectrics.[11] In addition to the corona charges in the voids in these foams, they usually also have to be inflated further with high pressure gas.[12] As a result, these ferroelectrets have long-term stability issues.[13]

Here, we demonstrate high converse piezoelectric response of fiber mats composed of ferroelectric barium titanate (BT) nanoparticles dispersed in polylactic acid (PLA) and show that the effective piezoelectric constant per weight is two orders of magnitude larger than that of single crystal BT and of pure piezoelectric ceramic fibers. We propose that this unexpected super-piezoelectricity is due to the electrospinning—induced polar alignment of the particles, and the large surface area of the fibers, similar to ferroelectrets, however without the need of corona discharge and inflation processes.

Electrospun fibers are formed by drawing a solution through a high electric field gradient generated between a nozzle and a collection plate[14–17] by electric fields of about 1-2 kV/cm, which is smaller than the breakdown field of 3 kV/cm of dry air. This produces very thin fibers with diameters ranging from hundreds of nanometers to several microns. Previously fibers of ferroelectric polymers, such as polyvinylidene fluoride (PVDF), have been electrospun and studied for electro-mechanical energy conversion applications.[18–21] Several examples of ferroelectric ceramic nanofibers have been fabricated using a sol-gel in the electrospinning process.[22–24] While the direct piezoelectric responses of ceramic fibers were demonstrated,[25,26] they are brittle. This problem was recently addressed by electrospinning of multi-material piezoelectric polymer fibers containing ferroelectric polymer PVDF.[27] Recently, electrospun nano-fibrous polymer films containing BT nanoparticles have been evaluated as possible dielectric materials for high capacitor applications,[28] but their piezoelectric properties have not been studied yet.

For the polymer matrix, we chose PLA because it has been used extensively for electrospun fibers, and it is biocompatible. BT nanoparticles are ferroelectric, readily available, and have also been well studied.

The details of the electro-spinning of the *PLA*/*BT* fibers (10-14) are described in supplementary material.[35] Figure 1 illustrates the experimental procedure, fiber structure, and the physical model of the piezoelectric response of the PLA/BT fibers. The solution, containing the PLA and BT particles, was pumped through a needle and drawn by the potential differences between the needle and the collector plate. In our work, we used a conducting indium tin oxide (ITO) coated glass [Figure 1(a)] for the collector plate. The nanostructure of the fiber, including BT particles, is shown in Figure 1(b), where the dark areas correspond to the particles. A mat of the fibers forms on the collector plate. The mat was sandwiched between the collector glass and a second ITO coated glass. The two glass substrates were used to apply an electric field across the fiber mat [Figure 1(c)].

The bottom glass substrate of the cell was fixed to the microscope stage and only the top substrate was able to move. A schematic of the set-up is shown in Figure S3 of supplementary material. First, we studied pure PLA fibers and PLA/BT films cast from solution. As discussed in Sec. IV of supplementary material, these samples show only electrostatic stress that is independent of the sign of the electric field. Then we measured the electric field-induced change of the thickness of mats of PLA/BT fibers at room temperature. The results are illustrated in Figures 2 and 3 for DC and AC voltages, respectively. The PLA/BT fiber mats respond linearly to the applied field, i.e., they expand or compress

a)Electronic mail: ajakli@kent.edu.

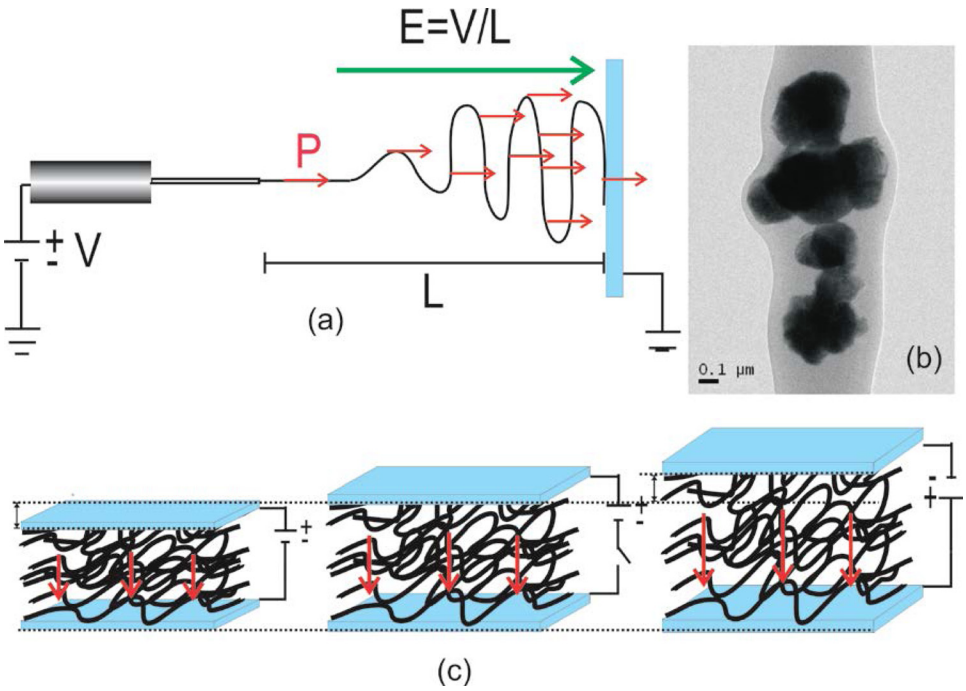

FIG. 1. (Color online) Illustration of the experimental procedures, fiber structure, and the physical model of piezoelectric response of the PLA/BT fiber mat: (a) Sketch of the standard electro-spinning process and poling; (b) TEM nanostructure of a fiber including BT particles (dark areas); and (c) sketch of the piezoelectric response when the external field is parallel, zero, and anti-parallel with the polarization of the BT nanoparticles, from left to right.

depending on the polarity of the applied field. The linear component disappears after the samples are heated above the Curie temperature, T_C, of BT. These clearly show that the aligned ferroelectric polarization of the BT is responsible for the linear electromechanical (piezoelectric) response.

The displacements of the top plate (Δd) were fit by the equation $\Delta d = \gamma \cdot V + \lambda \cdot V^2$, where γ is the piezoelectric coupling constant, and λ is the quadratic coupling constant. Figure 2 shows that in nm/V units $\gamma = 0.73$, 1.23, and 1.98 for the 110 ± 10 μm (o), 190 ± 10 μm (□), and 260 ± 10 μm (Δ) thick mats, respectively. Interestingly, the largest γ value published for single crystal BT films is $\gamma = 0.18$ nm/V, independent of the film thickness,[29] i.e., 4, 7, and 11 times smaller than we found for our mats, respectively.

Since the mass density of the fiber mat is only about 0.3 g/cm^3, whereas the BT is 5.9 g/cm^3; the converse piezoelectric response per unit weight of our composite materials is two orders of magnitude greater than of the single crystal BT.

The quadratic coupling constant λ in nm/V^2 units is 1.53×10^{-3}, 3.31×10^{-3}, and 5.54×10^{4} for the 110, 190, and 260 μm thick mats, respectively. In contrast to the converse piezoelectric response, the quadratic response does not disappear above the Curie temperature, because it is due to the electrostatic attraction stress, $\sigma_E = \frac{1}{2}\varepsilon.\varepsilon_0 E^2$ ($\varepsilon_o = 8.85 \times 10^{-12}$ C/(Vm) is the permittivity of the vacuum, and ε is the relative dielectric constant of the material). Equating σ_E with the elastic stress $\sigma_Y = Y \cdot \frac{\Delta d}{d}$, where Y is the compression modulus of the fiber mat, we get $\Delta d = \frac{\varepsilon_0 \varepsilon V^2}{2Yd}$. We measured the compression modulus and the relative dielectric constant (see Secs. III D and III E of supplementary material), and found that Y $\sim$ 16 kPa and $\varepsilon = 1.1 \pm 0.1$.

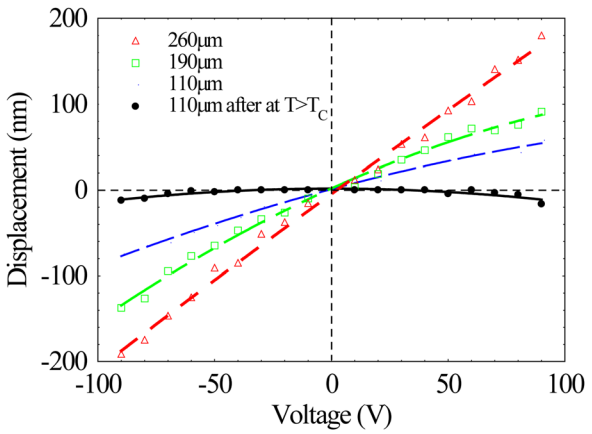

FIG. 2. (Color online) Measured displacements of the top plates of PLA/BT fiber mats with different thicknesses sandwiched between ITO-coated glass substrates versus applied DC voltage. All measurements were obtained at room temperature (23 °C). Dotted lines are fit to the fibers that have never been heated above the Curie temperature, and the solid line is a fit to the 110 μm thick film kept above the Curie temperature at T = 130 °C for 1 h. The fit equation in each case is $\Delta d = \gamma \cdot V + \lambda \cdot V^2$. The error of the measurements of the film thicknesses is ± 10 μm.

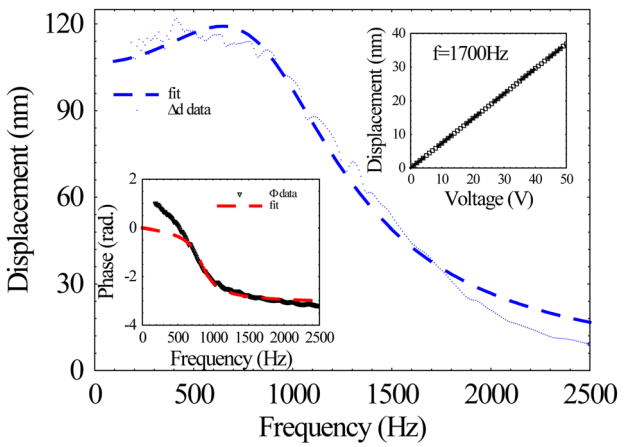

FIG. 3. (Color online) Frequency dependence of the displacement of the cover glass plate of $m_g = 2.5$ g measured by a $m_a = 2.5$ g accelerometer at 50 V applied, and of the fit of a forced damped oscillator (dotted line). Right upper inset: the voltage dependence of the displacement at 1700 Hz. Left lower inset: The frequency dependence of the phase in radians and a fit (dotted line).

This gives $\Delta d \sim 22$ nm at $V = 100$ V, which is comparable with the measured $\Delta d = 16$ nm, (see solid line in Figure 2).

Applying AC voltages above 20 Hz the vibration of the top plate was audible below about 1500 Hz. We measured the frequency dependence of the vibration amplitude of the top plate as described in Sec. III B of supplementary material. The frequency dependence of the amplitude Δd and phase Φ of the vibration are shown in Figure 3.

The frequency dependence can be fitted by the equations of a forced over-damped oscillator, $\Delta d = \frac{\Delta d_0}{\sqrt{(1-(f/f_o)^2)^2+(\xi f/f_o)^2}}$, $\Phi = \tan^{-1}\left(\frac{\xi(f/f_o)}{1-(f/f_o)^2}\right)$. Here $\omega_0 = 2\pi f_o = \sqrt{\frac{D}{m}}$, where the spring constant D is related to Y as $Y = D \cdot d/A$. As the total mass of the cover plate with the accelerometer is $m \sim 5$ g, from the best fit with $f_o \sim 800$ Hz we get $Y = 10^5$ N/m^2. This is about 6 times larger than the modulus we measured at *DC* voltages (see Sec. III D of supplementary material). The difference is probably due to the stiffening of the material with increasing frequencies, which would also explain why the fit to the displacement at high frequencies (see Figure 3) deviates slightly from the measured values.

The high converse piezoelectric-type responses presented above require that the BT particles are uniformly aligned and poled in the fiber. The particles are likely aligned by the electric field inherent in the electro-spinning process. The BT particles can easily rotate during the initial stages of the spinning process before the solvent completely evaporates. Evaporation of the solvent, and the hardening of the PLA around the BT particles lock in the orientation of the polarization of the particles normal to the collection plate. [Figure 1(a)]. Just as for the ferroelectrets, if a voltage is applied to the electrodes, the effective dipoles of the aligned BT particles contract or lengthen by moving the fibers closer or further from each other. The resulting apparent piezoelectricity of these particles causes the fiber mat to expand or compress when $\vec{P}$ is parallel or anti-parallel to the electric field $\vec{E}$ [see Figure 1(c)]. In continuous films, the bound charges of the electric polarization appear only at the surfaces. Consequently, the piezoelectric coupling constant is independent of the film thickness and the field-induced deformation is proportional to the voltage ($\Delta d = \gamma \cdot V$) if $\Delta d \ll d$. In the mats, the bound electric charges appear on the surfaces of the individual ferroelectric particles. Therefore, the total surface area—and consequently the effective piezoelectric constant—increases with the thickness of the mat, just as observed experimentally. Approximating the barium titanate particles by cubes with $a = 100$ nm sizes (see Figure 1), and assuming they all are separated by the polymer, the total surface area facing normal to the electric field is $N \cdot a^2$, where the number of particles N can be calculated by knowing that the volume of the particles is 1% of the volume of the whole sample that was 8×10^{-8} m^3 for the 200 μm mat. This gives $N = 8 \times 10^{11}$, i.e., a total area of 80 cm^2, which is 20 times larger than of the bounding plate. This means three times larger effective piezoelectric constant than the 7 fold increase observed experimentally. This is probably because some particles stick together as shown in Figure 1(b), thus decreasing the effective surface area.

The efficiency of our experimental fiber mats can be estimated by the ratio of the useful work done on the cover plate $W_u = m \cdot g \cdot h + \frac{1}{2} m \cdot h^2 \omega^2$, and of the electrical energy $W_E = \frac{\varepsilon_0 \varepsilon V^2 A}{2d}$ pumped in the sample. With the mass of $m = 2.5$ g, $h = 200$ nm at $V_{DC} = 100$ V and with $\varepsilon = 1.1$, we get 5% efficiency, which would increase with increasing load, as the compression and extension losses of the fiber mat would decrease with smaller displacements.

To summarize, we developed stimuli-responsive electrospun fibers that incorporate ferroelectric barium titanate particles. The apparent piezoelectric constant of the mats formed from these fibers is proportional to the mat thickness d, and for $d = 0.2$ mm, the displacements are about an order of magnitude larger than in single crystal BT films. The physical origin of this apparent super-piezoelectricity is basically the same as the charged polymer foams with the important difference that here the poling is not due to corona discharge, but is the result of poling the ferroelectric particles during the electro-spinning process. We note that tetragonality and therefore the piezoelectric coupling constant may change with the size of the particles,[30,31] so the ratios of the effective surface areas are not necessarily the only factor determining the effective piezoelectric constant. Other effects, such as interfacial piezoelectricity[32,33] may also contribute to the apparent piezoelectricity of the composite fiber mat of our studies. Importantly, the compression modulus of the mats is similar to that of biological cell tissues (such as muscles, liver, loin),[34] simplifying matching mechanical impedances that will provide the highest energy conversion efficiency. The fiber mats are lightweight and the PLA is biocompatible, offering a myriad of applications ranging from active implants, artificial muscles, sensors, to textiles that contract or expand upon application of an electric field.

The TEM picture was obtained at the cryo-TEM facility at the Liquid Crystal Institute, Kent State University, supported by the Ohio Research Scholars Program "Research Cluster on Surfaces in Advanced Materials." The authors would like to thank Professor Margaret Frey, Cornell University for PLA resins, Dr. J. Harden for helpful discussions, and Liou Qiu, Kent State University for her assistance in the SEM characterization of the samples.

[1]J. Curie and P. Curie, Bulletin no. 4 de la Societee Mineralogique de France **3**, 90 (1880); Acad. Sci., Paris, C.R. **91**, 29 (1880).
[2]B. M. Wul and I. M. Goldman, Akad. Nauk. **49**, 179 (1945); A. Von Hippel, R. G. Breckenridge, F. G. Chesley, and L. Tisza, Ind. Eng. Chem. **38**, 1097 (1946); S. Roberts, Phys. Rev. **71**, 890 (1947).
[3]H. Kaway, Jpn. J. Appl. Phys. **8**, 975 (1970).
[4]Y. Wada, in *Electronic Properties of Polymers*, edited by J. Most and G. Pfister (Wiley-Interscience, New York, 1982), Chap. 4.
[5]E. Fukada, Adv. Biophys. **6**, 121 (1974).
[6]P. Pieranski, E. Guyon, and P. Keller, J. Phys. **36**, 1005 (1975).
[7]A. Jákli, L. Bata, Á. Buka, N. Éber, and I. Jánossy, J. Phys. Lett. **46**, L-759 (1985).
[8]P. Langevin, French patent 505,703 (17 September 1918).
[9]W. G. Cady, Phys. Rev. **27**, 419 (1915).
[10]Y. Dzenis, Science **304**, 1917 (2004).
[11]J. Lekkala, R. Poramo, K. Nyholm, and T. Kaikkonen, Med. Biol. Eng. Comput. **34**, 67 (1996).
[12]G. M. Sessler and J. Hillenbrand, Appl. Phys. Lett. **75**, 3405 (1999).
[13]S. Bauer, R. Gerhard-Multhaupt, and G. M. Sessler, Phys. Today **57**, 37 (2004).

[14]C. Huang, S. Chen, C. Lai, D. H. Reneker, H. Qiu, Y. Ye, and H. Hou, Nanotechnology **17**, 1558 (2006).
[15]D. H. Reneker and A. Yarin, Polymer **49**, 2387 (2008).
[16]G. C. Rutledge and S. V. Fridrikh, Adv. Drug Delivery Rev. **59**, 1384 (2007).
[17]A. Greiner and J. H. Wendorff, Angew. Chem., Int. Ed. **46**, 5670 (2007).
[18]S. Huang, W. A. Yee, W. C. Tjiu, Y. Liu, M. Kotaki, Y. Chiang, F. Boey, J. Ma, T. Liu, and X. Lu, Langmuir **24**, 13621 (2008).
[19]C.-C. Wang, J.-F. Song, H.-M. Bao, Q.-D. Shen, and C.-Z. Yang, Adv. Funct. Mater. **18**, 1299 (2008).
[20]Y. Liu, Y. Li, J.-T. Xu, and Z.-Q. Fan, Appl. Mater. Interfaces **2**, 1759 (2010).
[21]J. S. Andrew and D. R. Clarke, Langmuir **24**, 670 (2008).
[22]S. H. Xie, J. Y. Li, Y. Y. Liu, L. N. Lan, G. Jin, and Y. C. Zhou, J. Appl. Phys. **104**, 024115 (2008).
[23]Y. Wang, R. Furlan, I. Ramos, and J. J. Santiago-aviles, Appl. Phys. A **78**, 1043 (2004).
[24]X. Chen, S. Xu, N. Yao, and Y. Shi, Nano Lett. **10**, 2133 (2010).
[25]J. Yuh, J. C. Nino, and W. M. Sigmund, Mater. Lett. **59**, 3645 (2005).
[26]Z. Wang, J. Hu, A. P. Suryavanshi, K. Yum, and M. Yu, Nano Lett. **7**, 2966 (2007).
[27]S. Egusa, Z. Wang, N. Chocat, Z. M. Ruff, A. M. Stolyarov, D. Shemuly, F. Sorin, P. T. Rakich, J. D. Joannopoulos, and Y. Fink, Nature Mater. **9**, 643 (2010).
[28]B. Carlberg, J. Norberg, and J. Liu, in *Proceedings of the 57th Electronic Components and Technology Conference* (IEEE, 2007), pp. 1019-1026.
[29]S. Wada, S. Suzuki, T. Noma, T. Suzuki, M. Osada, M. Kakihana, S.-E. Park, L. Cross, and T. Shrout, Jpn. J. Appl. Phys. **38**, 5505 (1999).
[30]A. L. Yarin, S. Koombhongse, and D. H. Reneker, J. Appl. Phys. **89**, 3018 (2001).
[31]Y. Yamamoto, Jpn. J. Appl. Phys. **32**, 4272 (1993).
[32]E. Fukada, IEEE Trans. Ultrason., Ferroelectr. Freq. Control **47**(6), 1277 (2000).
[33]C. K. Wong and F. G. Shin, J. Appl. Phys. **97**, 034111 (2005).
[34]V. Egorov, S. Tsyuryupa, S. Kanilo, M. Kogit, and A. Sarvazyan, Med. Eng. Phys. **30**(2), 206 (2007).
[35]See supplementary material at http://dx.doi.org/10.1063/1.3683482 for composition, description of the measurements techniques, and characterization of some parameters.